



**WESTERN REGION TECHNICAL ATTACHMENT
NO. 96-12
June 25, 1996**

**AN EVALUATION OF THE PERFORMANCE OF
THE MESO-ETA MODEL ON A DYNAMIC COLD SEASON
BOW ECHO IN CALIFORNIA**

**Mike Staudenmaier, Jr.
SSD/NWSFO Salt Lake City, UT**

Introduction

On 1 April 1996, a well developed bow echo developed over the northern San Joaquin Valley of California. This bow echo, and a weaker bow echo to the south, moved rapidly to the east-northeast at around 40-45 mph with damage paths oriented from south-southwest to north-northeast along the strongest portion of each bow echo. An investigation of the WSR-88D data along with mesoscale analyses was completed by the author (Staudenmaier and Cunningham, 1996), which demonstrated that this bow echo had the typical mesoscale structures which have been documented in bow echoes occurring east of the Rocky Mountains. It was also shown that local topography appeared to play a crucial role in the initial development and location of the bow echoes. This Technical Attachment will investigate the performance of the Meso-Eta model in predicting the development, location, and propagation of this bow echo complex.

Background

Squall lines have long been recognized as severe weather producers. Occasionally, these systems developed a bulging, convex shape (as depicted by radar) and were accompanied by stronger surface winds. Fujita (1981) described the basic morphology and evolution of this particular type of storm, which he classified as a bow echo. For more information regarding bow echoes and specific information regarding the 1 April 1996 event, the reader is urged to read Staudenmaier and Cunningham (1996). Information regarding the Meso-Eta model can be found in Staudenmaier (1996).

Performance of The Meso-eta

As described in Staudenmaier and Cunningham, the synoptic pattern on 1 April 1996 was characterized by a moderately strong cold frontal passage south of an area of synoptic low pressure which was producing moderately strong vertical wind shear in a weakly stable environment. This synoptic pattern resembled the "classic" California severe weather pattern as convection occurred behind a weakening, mainly upper-level, front but before

a secondary, and strengthening, frontal feature moved across the state. Conditionally unstable air remained in the lower levels following the passage of the weak upper-level front, while cold air advection aloft destabilized the airmass further. Clouds covered much of the region due to the synoptic-scale lift occurring over the state, but breaks in the cloud cover over portions of the San Joaquin Valley allowed temperatures to climb into the 60s by early afternoon with dewpoint temperatures remaining in the middle and upper 50s. By 1800 UTC, scattered areas of convection were beginning to develop along the secondary cold front as it moved towards the California coast.

A 0.5 degree base reflectivity scan at 2152 UTC from the Sacramento WSR-88D (Fig 1) shows the developing squall line over the western portions of the San Joaquin Valley with a slight bow structure already occurring southwest of the city of Stockton. A graphic of 3-hourly convective rainfall totals from the Meso-Eta model (Fig 2) indicated that the model had developed a line of convection along the coast and with an assumed westward movement, this line could be inferred to be located over the extreme western portion of the San Joaquin Valley at around the same time. This location is strengthened by the convergence located in the lowest level wind field from the Meso-Eta for 2100 UTC (Fig 3). The wind flow ahead of the convective line was from the south-southeast at 10-20 mph which compares very well with the observed wind field. Westerly winds behind the frontal feature of 10-15 mph were much weaker than the 15-30 mph sustained winds which were actually reported. Much stronger westerly wind gusts of over 55 mph were associated with the actual track of the bow echo.

Associated with this wind shift at the surface was a push of drier and cooler air associated with a mid-level jet streak rotating around the base of the trough of low pressure. A 21 hour model forecast cross-section from San Francisco, CA (SFO) to Lander, WY (LND) at 0000 UTC 2 April (Fig 4) clearly showed this feature as much lower theta-e values were being advected into the rear portion of the model-produced convective complex. A nose of stratospheric air can also be seen over this theta-e minimum, associated with the synoptic scale trough aloft. The convective line was modeled to be over the Sierra Nevada Mountains at 0000 UTC, which again, verified well with reality.

At the surface, the pre-bow echo pressure pattern in the model forecast also closely resembled reality. At 2100 UTC, the Meso-Eta had developed a weak area of higher pressure near the Sierra Nevada Mountains, with a trough of low pressure oriented along the western portion of the San Joaquin Valley (Fig 5). High pressure could be seen pushing southward over the Sacramento Valley. A meso-analysis for the same time period (Fig 6) shows a similar pressure pattern with high pressure over the Sacramento Valley and a trough of low pressure over the western portion of the San Joaquin Valley. The meso-high located near Travis AFB (SUU) was likely caused by rain-cooled air. However, the Meso-Eta model did not capture any of the low level meso-scale features of the convective complex itself once it matured, including the wake low and meso-high.

The Meso-Eta model performed moderately well on thermodynamics as well. Model-

generated Convective Available Potential Energy (CAPE) for 2100 UTC indicated that unstable air was located immediately along and behind the convective complex (Fig 7). Apparently the model did not stabilize the atmosphere significantly behind this convective complex, instead allowing the atmosphere to remain unstable. In addition, the model did not generate any Convective Inhibition (CIN) over this area to act as a cap on the instability. A modified sounding, attempting to approximate the pre-storm environment at Stockton (SCK), indicated that immediately before the complex moved over the station, CAPE values approached 250 J/kg (Fig 8). A thermodynamic profile created by the Meso-Eta shows a similar profile with only marginal instability (Fig 9). The wind shear profiles were similar as well, although the lowest winds in the model were slightly weaker than reality.

Other fields were also looked at, with similar results. The Meso-Eta captured the synoptic conditions leading up to the convective complex, but did not develop strong enough winds near the surface, both ahead and behind the complex. Reasons for this are many, but most likely the main reason was that the convective parameterization in the model did not mix momentum down to the ground, leading to a much less organized surface meso-scale pressure field. It has been shown that the meso-scale pressure patterns produced by the updraft/down draft couplet are important in both the propagation and continued development of an organized area of convection, along with significantly modifying the surrounding synoptic environment (LeMone and Moncrieff (1994) and Wu and Yanai (1994). Although synoptic features, such as the mid-level theta-e minimum, the modest instability, the moderately strong wind shear, and the jetstreak moving into the rear of the convective complex, were captured quite well, the lack of a mechanism for mixing momentum down to the surface led to a weaker and slower system than what actually occurred.

Additionally, no rear-inflow jet could be seen into the convective complex. Although the 700 mb field did indicate a synoptic area of higher winds into the rear portion of the complex, the convective parameterization and course grid spacing will never allow the development of book end vortices as were seen in reality. Thus, the enhancement in the wind field, both aloft and at the surface, which were produced by these vortices will not be captured thus leading to a slower and weaker solution.

Conclusion

The Meso-Eta model was investigated to see how well it performed during a convective event in California. It was found that the Meso-Eta did reasonably well in detecting the development of convection over the San Joaquin Valley of California, along with the organization of the precursor elements which led to the development of the bow echo complex. However, due to the parameterization of convection, the model did not develop the stronger meso-scale surface pattern which eventually developed in reality, leading to much weaker surface winds and lighter rains than actually occurred. The model appeared

to have a difficult time stabilizing the airmass behind the convective line as well, again likely due to insufficient mixing and stabilizing of the model atmosphere in the convective parameterization scheme. Forecasters should be encouraged by these preliminary results from the Meso-Eta however, since the diagnosis of the precursor severe weather environment is still a very important tool in anticipating severe weather. With better resolution anticipated in the Meso-Eta model, the diagnosis of the precursor severe weather environment should only get better.

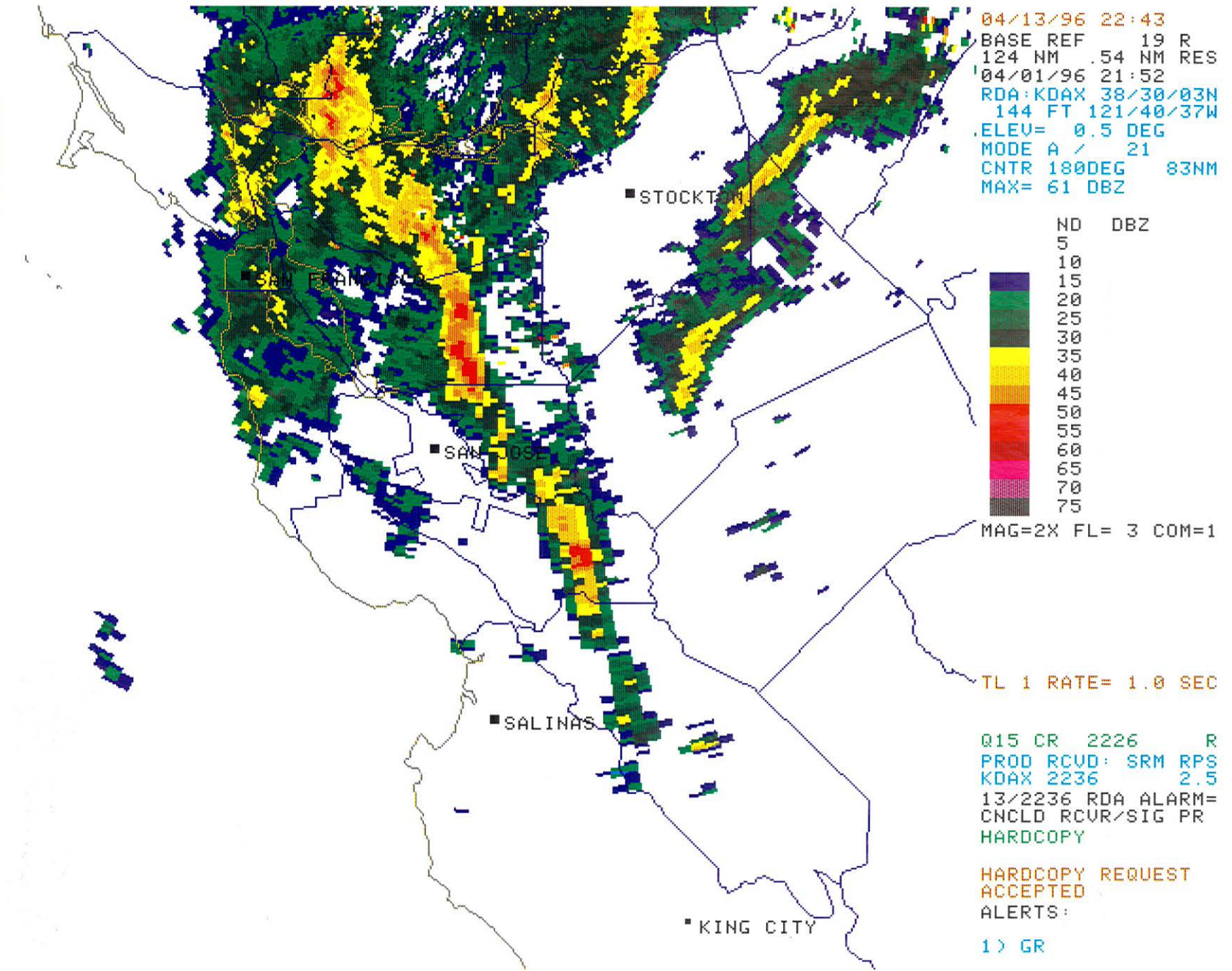
References

- LeMone, M.A., 1994: Momentum and mass transport by convective bands: Comparisons of highly idealized dynamical models to observations. *J. Atmos. Sci.* **51**, 281-305.
- Fujita, T.T., 1981 : Tornadoes and downbursts in the context of generalized planetary scales. *J. Atmos Sci*, **38**, 1511-1534.
- Staudenmaier, M.J. and S. Cunningham, 1996: An examination of a dynamic cold season bow echo in California. Western Region NWS Technical Attachment 96-10.
- Staudenmaier, M.J., 1996: A description of the Meso-Eta model. Western Region NWS Technical Attachment 96-06.
- Wu, X., and M. Yanai, 1994: Effects of vertical wind shear on the cumulus transport of momentum: Observations and parameterization. *J. Atmos. Sci.*, **51**, 1640-1660.

Figures

- Figure 1: 21:52 UTC 0.5 degree base reflectivity scan from the Sacramento WSR-88D on 1 April 1996.
- Figure 2: 3 hourly total precipitation (inches) from the Meso-Eta model for the period 1800-2100 UTC 1 April 1996.
- Figure 3: Lowest level wind field and topography from the Meso-Eta model valid at 2100 UTC 1 April 1996. Windspeed is in knots.
- Figure 4: Meso-Eta cross-section from San Francisco, CA (SFO) to Lander, WY (LND) at 0000 UTC 2 April 1996. Shaded values are Potential vorticity greater than 1.5 units, thick solid lines are theta-e, and dashed lines are relative humidity.
- Figure 5: Mean sea level pressure at 2100 UTC 1 April 1996 from the Meso-Eta model. Solid lines are pressure in millibars and dashed lines are 100-500 mb thickness in dm.
- Figure 6: Meso-scale analysis valid at 2100 UTC 1 April 1996. Solid lines are isobars contoured every .01 inches of mercury.
- Figure 7: Meso-Eta best Convective Available Potential Energy (CAPE) valid at 2100 UTC 1 April 1996.
- Figure 8: Modified thermodynamic profile for Stockton, CA (SCK) valid at 2200 UTC 1 April 1996.
- Figure 9: Meso-Eta derived thermodynamic profile for Stockton, CA (SCK) valid at 2100 UTC 1 April 1996.

Figure 1



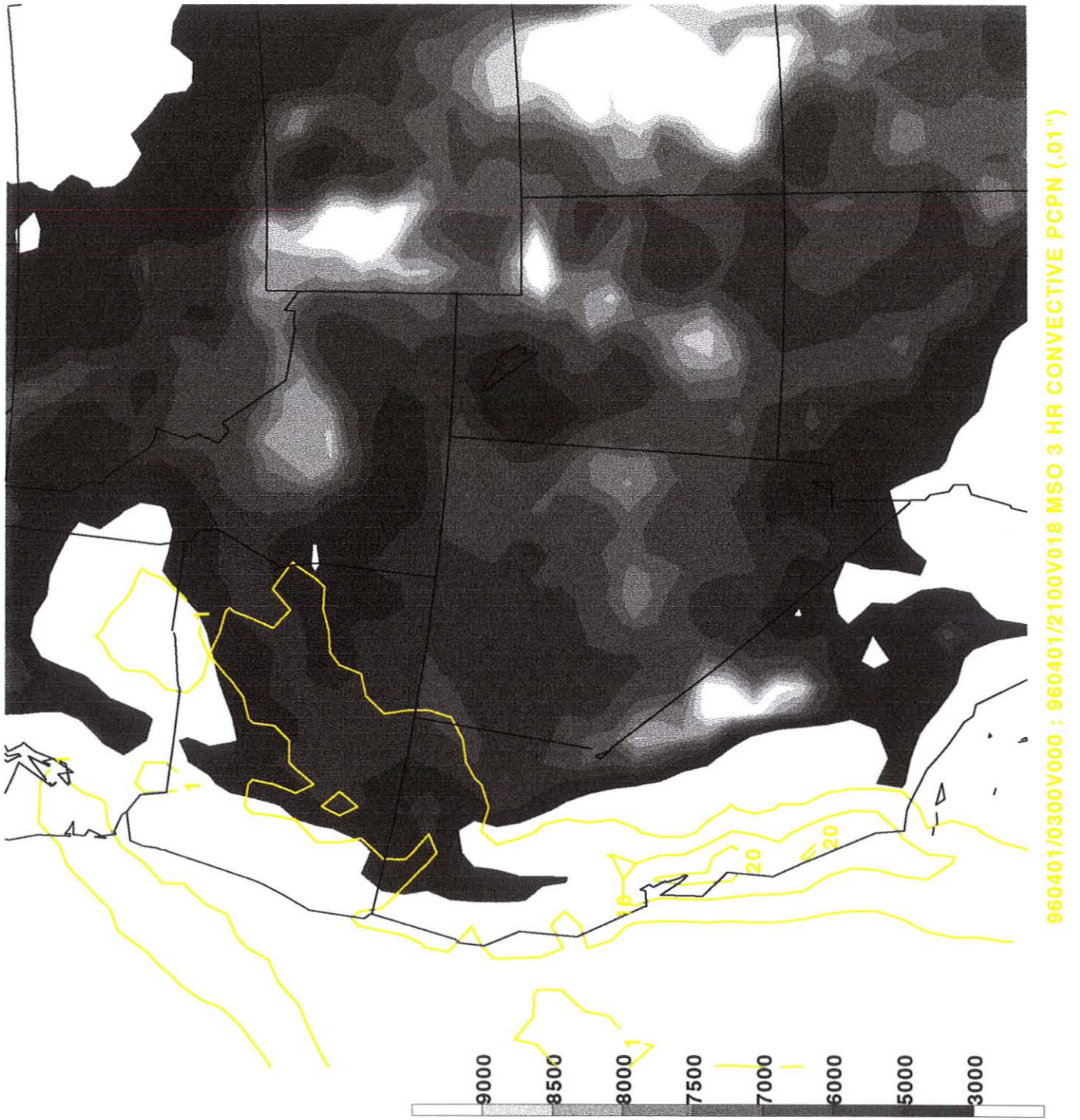
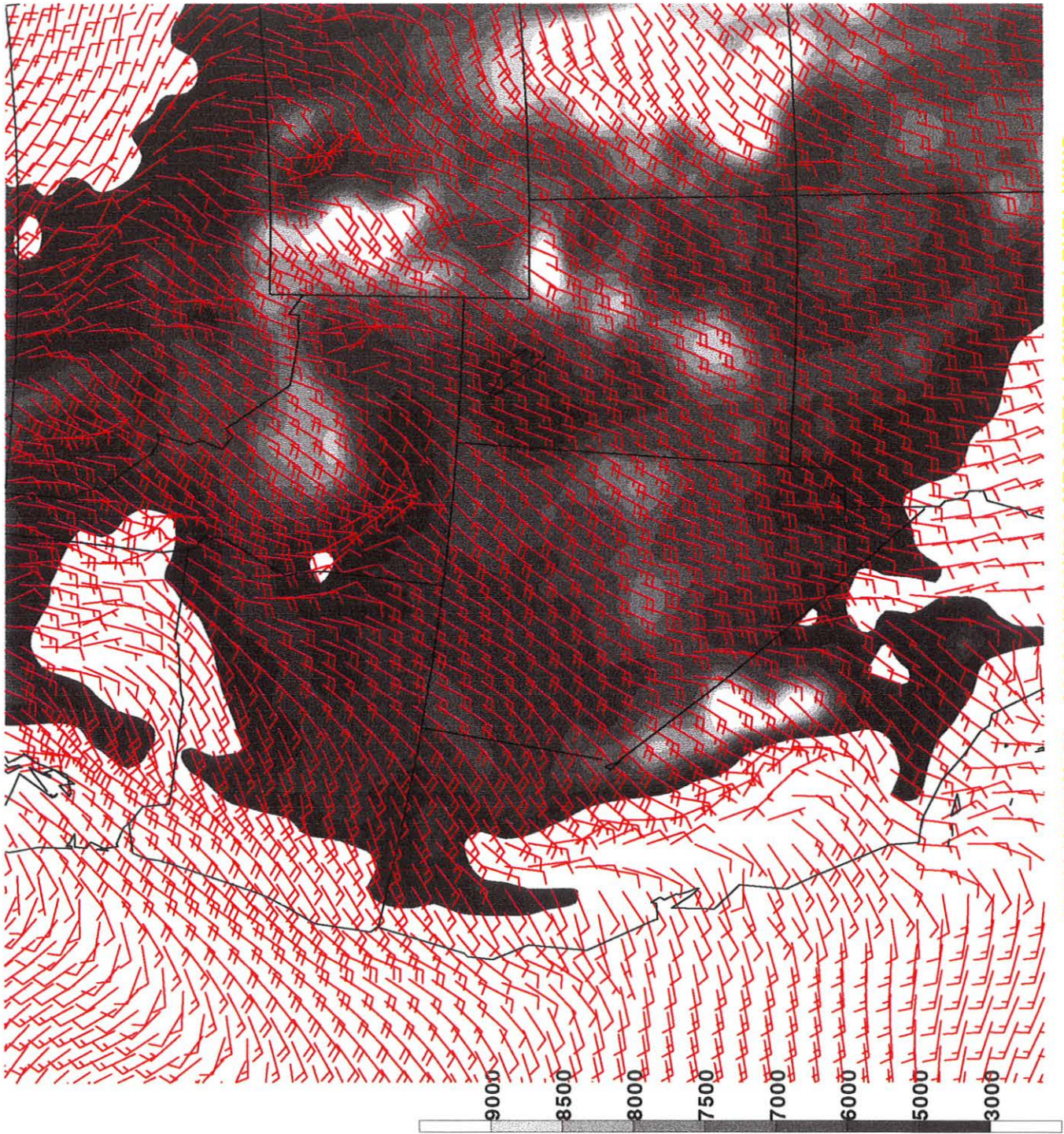


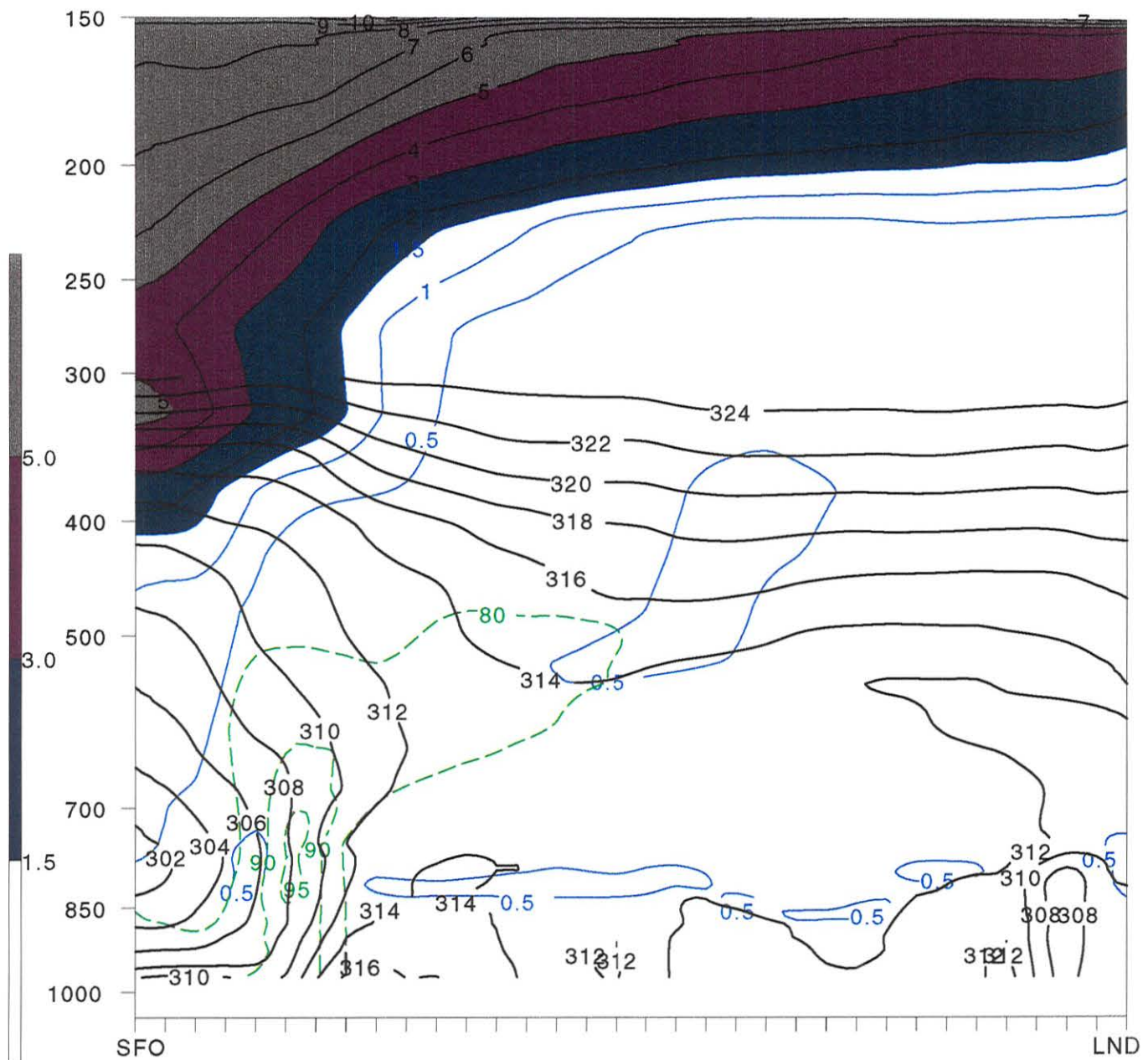
Figure 2



960401/0300V000 : 960401/2100V018 MESOETA LOWEST LEVEL WIND

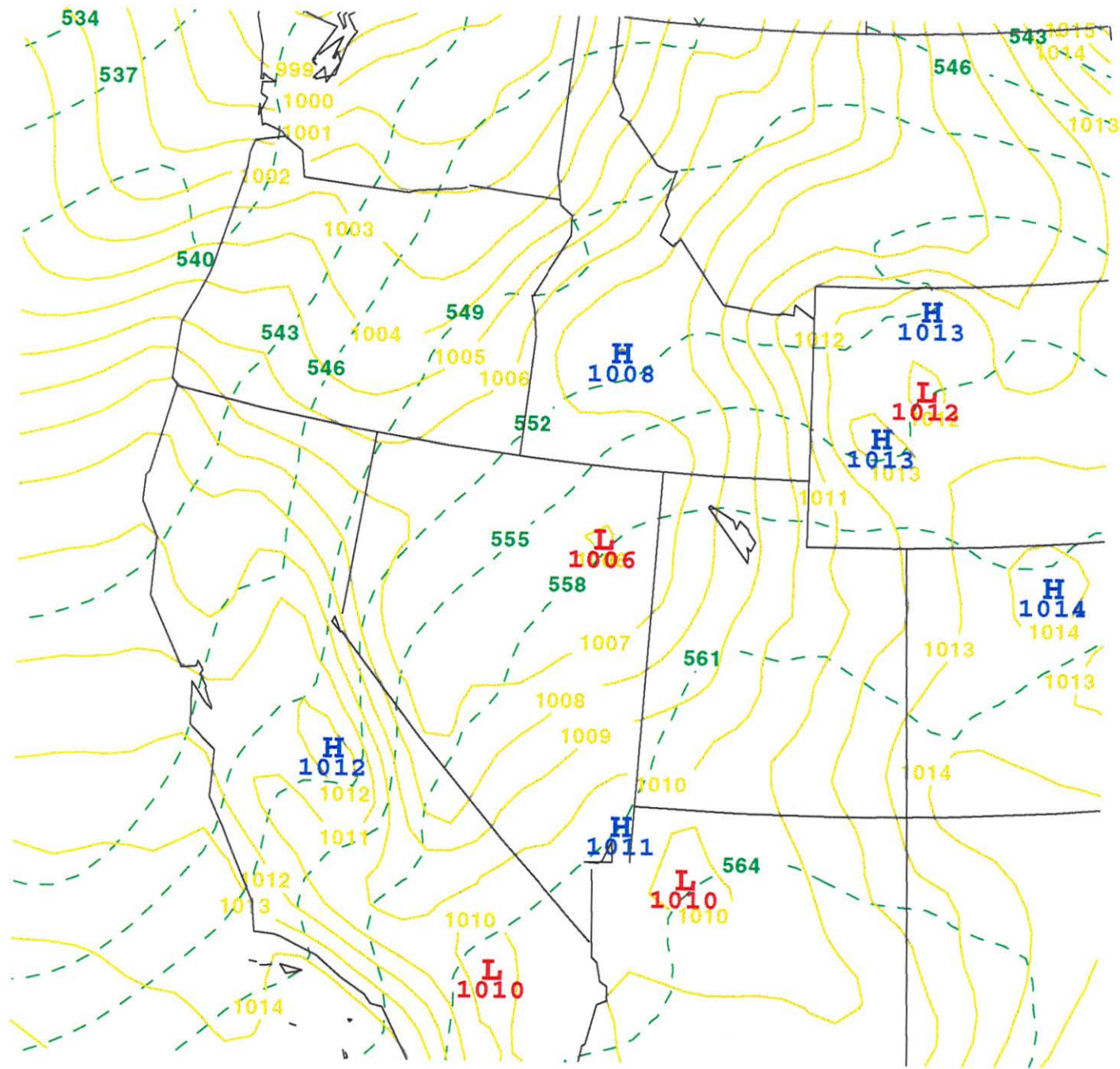
Figure 3

Figure 4



960402/0000V021 MSO THTA-E, RH, PV

Figure 5



960401/2100V018 MSO - MSLP & 1000-500mb THICK

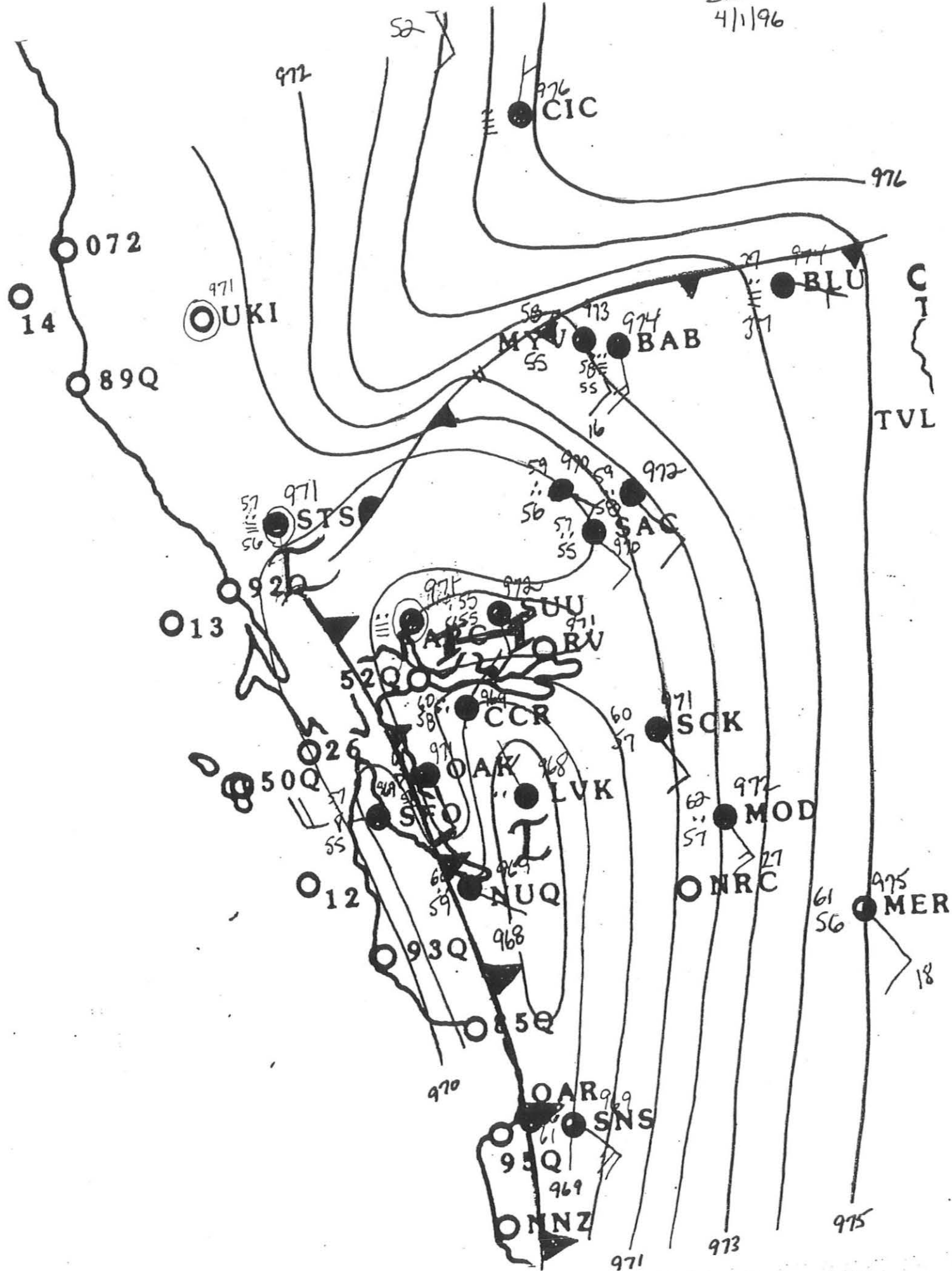


Figure 6

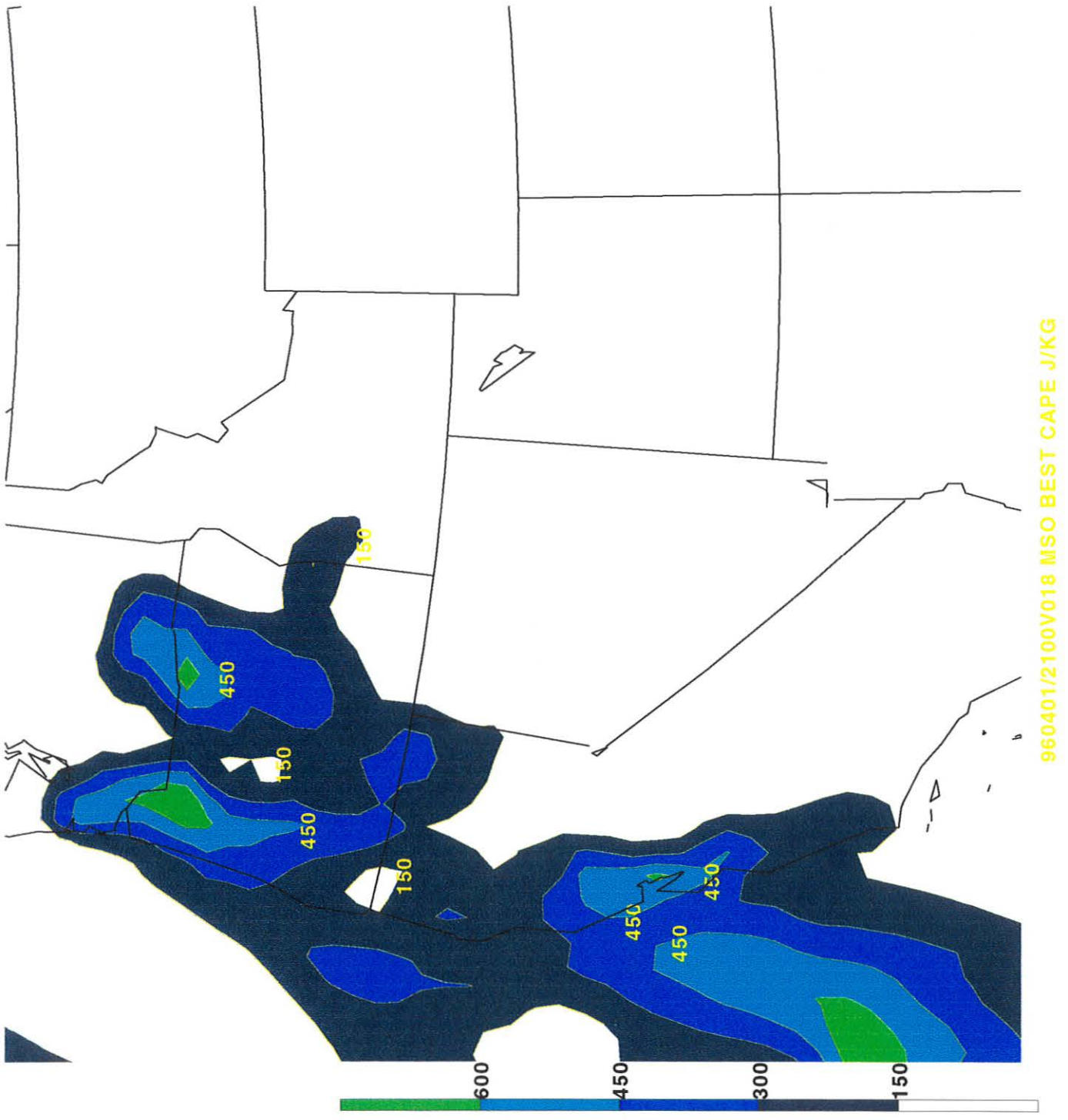


Figure 7

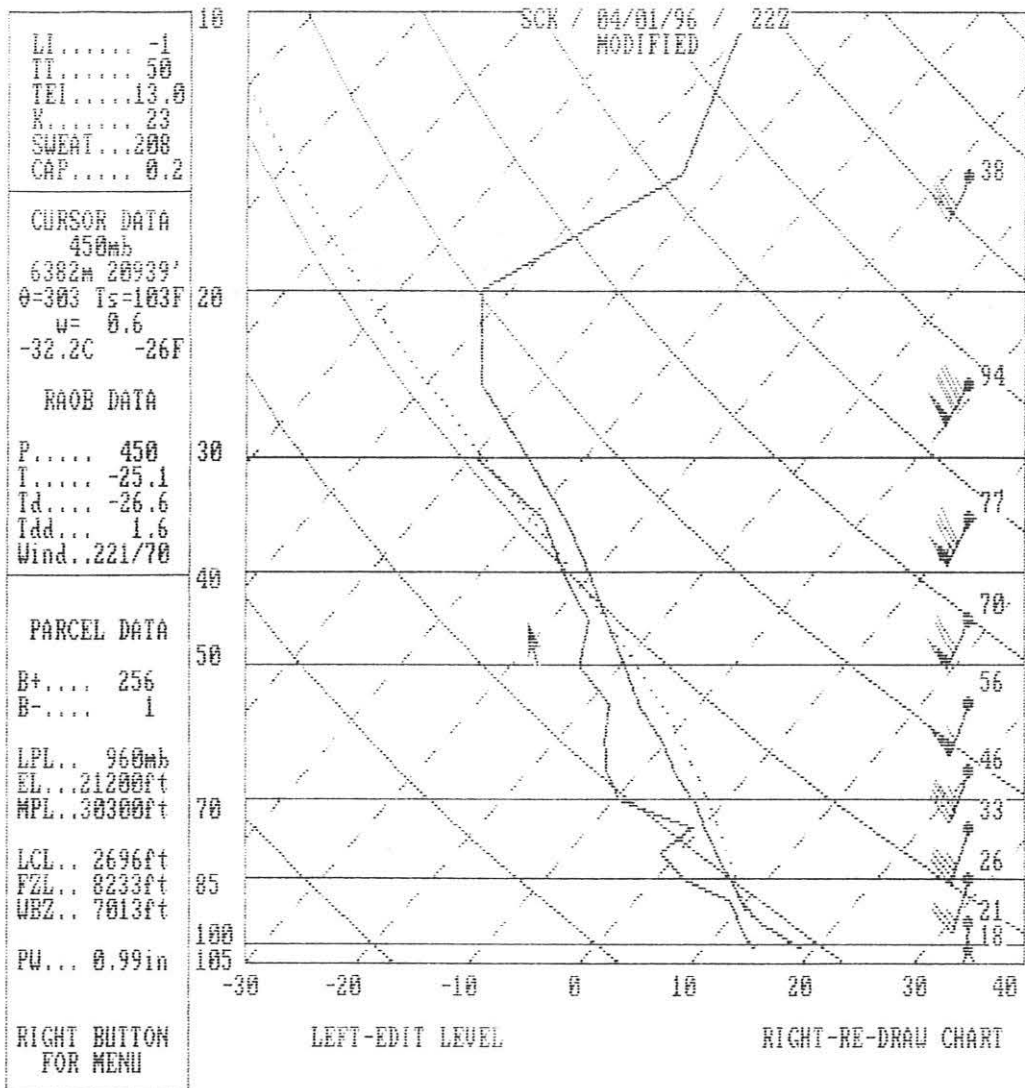


Figure 8

Figure 9

